

# Raman spectroscopic study of spodumene ( $\text{LiAlSi}_2\text{O}_6$ ) through the pressure-induced phase change from $C2/c$ to $P2_1/c$

C. J. S. Pommier,<sup>1</sup> M. B. Denton<sup>1</sup> and R. T. Downs<sup>2\*</sup>

<sup>1</sup> Department of Chemistry, University of Arizona, Tucson, Arizona 85721-0041, USA

<sup>2</sup> Department of Geosciences, University of Arizona, Tucson, Arizona 85721-0077, USA

Received 17 January 2003; Accepted 6 June 2003

High-pressure Raman spectroscopy was used to follow the effects of a phase transition on the Raman spectrum of a natural specimen of the pyroxene spodumene, from its low-pressure ( $C2/c$ ) to its high-pressure ( $P2_1/c$ ) phases. The transition occurred at 3.2 GPa and was accompanied by an increase from 15 to 23 observed peaks, owing to a decrease in symmetry. Comparisons were made with other pyroxenes with the same space groups. The change in Raman shift with pressure of all peaks observed is reported. An additional change in the spectrum is observed between 7.7 and 8.9 GPa, possibly due to the formation of an additional bond between Li and O3 or some other transition that retained the mineral's  $P2_1/c$  space group. Splitting of the peak appearing at  $\sim 700\text{ cm}^{-1}$ , used to characterize the  $P2_1/c$  phase in other studies, was not observed. Copyright © 2003 John Wiley & Sons, Ltd.

**KEYWORDS:** spodumene; pyroxene; pressure-induced phase change; high-pressure Raman spectroscopy

## INTRODUCTION

Spodumene ( $\text{LiAlSi}_2\text{O}_6$ ) is a monoclinic, optically biaxial member of the pyroxene group of minerals. Pyroxenes (general formula  $\text{M}_2\text{M}_1\text{Si}_2\text{O}_6$ ) comprise approximately 25% of the Earth's volume to a depth of 400 km.<sup>1</sup> There are a variety of symmetries exhibited by pyroxenes, most notably  $C2/c$ ,  $P2_1/c$ ,  $Pbca$  and  $Pbcn$ , and all pyroxenes appear to undergo phase transitions between these various symmetries as a function of pressure and temperature. The atomic scale mechanisms for these changes have been the subject of much study.<sup>2</sup> A recently discovered phase transition in pyroxenes, accompanied by a volume change, is now accepted as an origin of deep-focus earthquakes at a depth of about 225 km.<sup>3–5</sup> Spodumene is a principle source of lithium and has uses in the glass and ceramics industries. In spodumene, chains of  $\text{AlO}_6$  (M1) octahedra separate chains of  $\text{SiO}_4$  tetrahedra (Fig. 1). Li occupies the M2 site. In general, the M2 site is observed to be 4-, 5-, 6- or 8-coordinated, depending on pressure, temperature and composition. There are three symmetrically non-equivalent oxygens, designated O1, O2 and O3. O1 oxygens are at the apices of the  $\text{SiO}_4$  tetrahedra, O2 are on the base of the tetrahedra and O3

are on the base of the tetrahedra bridging the silicon atoms. Sharma and Simons have already reported the Raman spectra of three high-temperature polymorphs of spodumene and glasses of spodumene composition.<sup>6</sup> A recently discovered high-pressure phase of spodumene<sup>7</sup> was not one of the polymorphs studied.

Depending on temperature and pressure, spodumene has been observed in either  $C2/c$  or  $P2_1/c$  symmetry.<sup>7</sup> At pressures below 3.2 GPa, the mineral displays space group symmetry  $C_{2h}^6$  ( $C2/c$ ). In this phase, both Li and Al occupy positions of  $C_2$  site symmetries. The Si and all three types of oxygens display  $C_1$  site symmetry. According to factor group analysis, there are 14  $A_g$  and 16  $B_g$  Raman-active modes associated with the  $C2/c$  phase.

Near 3.2 GPa, the mineral undergoes a reversible phase transition to the  $C_{2h}^5$  space group ( $P2_1/c$ ).<sup>7</sup> At the transition, the coordination of the Li atom changes from 6 to 5 when the bond to the O3 oxygen atom in the 3-position breaks (see Fig. 1).<sup>2</sup> The loss of this bond destroys the  $C_2$  symmetry of the mineral. In the  $P2_1/c$  phase, all atoms in spodumene display  $C_1$  site symmetries. There should be 30 Raman-active  $A_g$  modes and 30  $B_g$  modes. The phase transition is accompanied by a 1.4% decrease in volume. This phase transition has been documented by x-ray diffraction studies.<sup>7</sup>

The Raman spectrum of spodumene in the  $P2_1/c$  phase has not yet been reported. It is the purpose of this paper

\*Correspondence to: R. T. Downs, Department of Geosciences, University of Arizona, Tucson, Arizona 85721-0041, USA.  
E-mail: downs@geo.arizona.edu

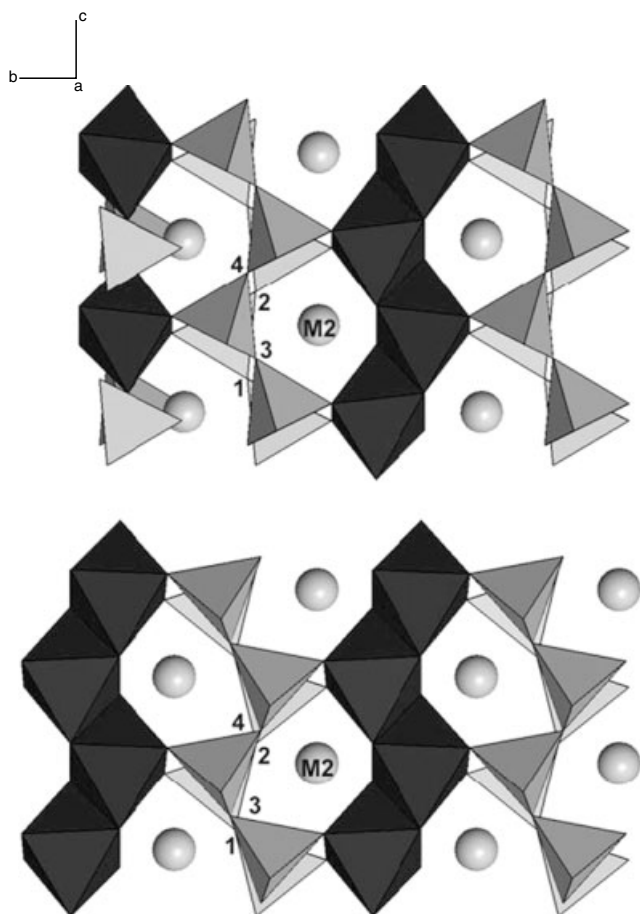


**Figure 1.** Top,  $C2/c$  spodumene structure, and bottom,  $P2_1/c$  spodumene structure. Solid lines illustrate Li–O bonds. The dotted line illustrates the bond that appeared at 8.84 GPa in Ref. 7.

to demonstrate the changes in the Raman spectrum of spodumene that are indicative of the phase transition from  $C2/c$  to  $P2_1/c$  and to compare the Raman spectra of these phases with similar phases in other pyroxenes. It is becoming apparent that the transformations between pyroxenes that display  $C2/c$ ,  $P2_1/c$ ,  $Pbca$ ,  $Pbcn$  and  $P2_1cn$  ( $C_{2h}^6$ ,  $C_{2h}^5$ ,  $D_{2h}^{14}$ ,  $D_{2h}^{15}$ ,  $C_{2v}^9$ ) symmetries are much more common than previously thought. As such, an additional purpose of this paper is to establish a method to characterize the different symmetries using Raman spectroscopy.

## EXPERIMENTAL

The sample was a fragment of a large, pale pink gem crystal from Pala, San Diego County, CA, USA. The  $200 \times 200 \times 25 \mu\text{m}$  fragment was loaded into a four-pin Merrill Basset-type diamond cell with (110) parallel to the cell axis. The diamond anvil culet size was  $600 \mu\text{m}$ . A stainless-steel gasket,  $250 \mu\text{m}$  thick, pre-indented to  $50 \mu\text{m}$ , with a hole diameter of  $300 \mu\text{m}$  was used. The cell was loaded

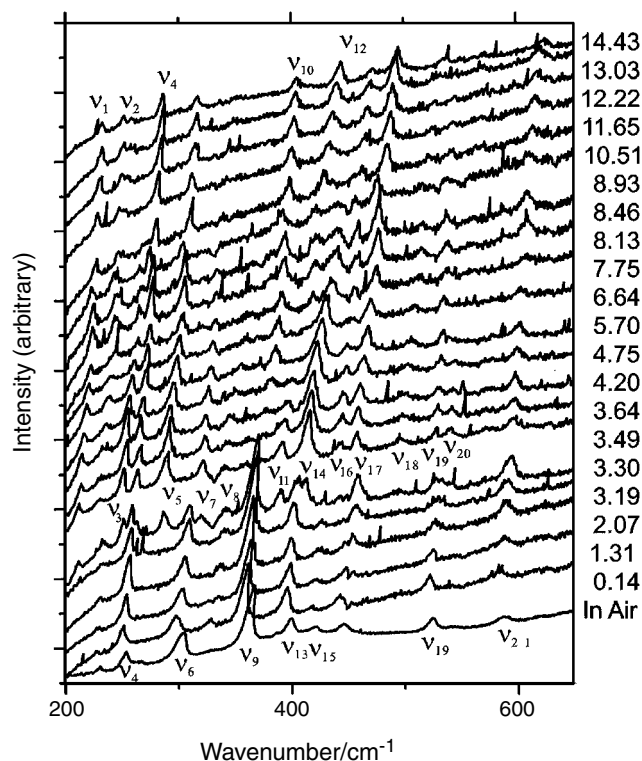


**Figure 2.** Low-wavenumber region of spectra as the pressure is varied. Note the spectrum at 3.30 GPa where both phases are evident and the change in spectra between 7.75 and 10.51 GPa.

with the spodumene crystal and a small ruby fragment, and filled with 15:4:1 methanol–ethanol–water pressure medium. Pressures were determined from fitted positions of the  $R_1$  and  $R_2$  ruby fluorescence spectra using the calibration of Mao *et al.*<sup>8</sup> The error in pressure is estimated to be 0.05 GPa. Pressure was measured before and after each spectrum acquisition and the reported value is the average of these two measurements. Both ruby fluorescence and Raman spectra were excited with a 514.5 nm argon ion laser.

There was no specific polarization alignment along the crystal the axes. Raman scattering was collected in the backscattered geometry. Rayleigh scattering was filtered out using two Kaiser Optics holographic filters. Spectra were acquired using a Jobin Yvon Spex HR 460 spectrometer and a liquid nitrogen-cooled  $1152 \times 256$  pixel Princeton Instruments charge-coupled device (CCD) detector. Utilizing an  $1800 \text{ grooves mm}^{-1}$  grating centered at 530 nm, the region from  $104$  to  $1010 \text{ cm}^{-1}$  was acquired using WinSpec software. However, owing to interference from the filters, only the region above  $200 \text{ cm}^{-1}$  was analyzed. Data were imported into GRAMS 32 software and peak positions were found using the peak fitting utility. Errors averaged less than  $1 \text{ cm}^{-1}$  for all peak positions with the errors for most peaks falling well below  $1 \text{ cm}^{-1}$ .

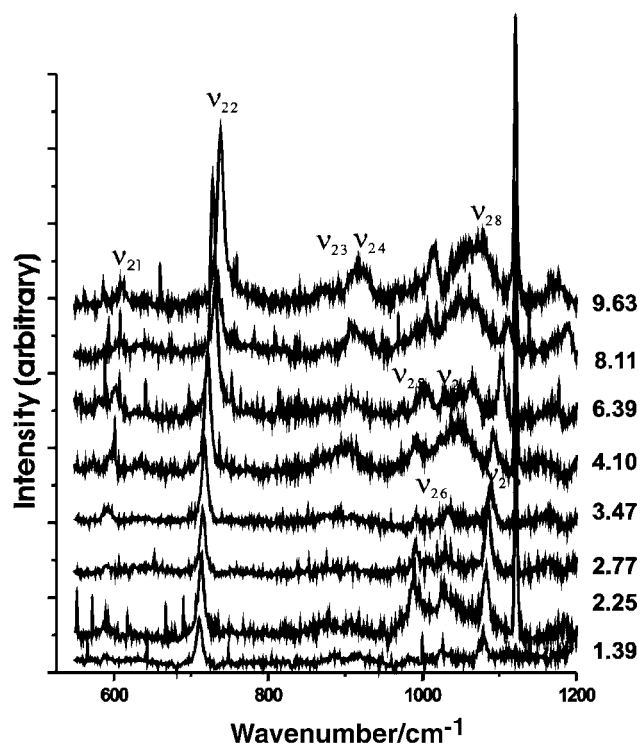


**Figure 3.** High-wavenumber region of spectra as pressure is decreased. The peak at  $1119\text{ cm}^{-1}$  represents interference from monitors in the room, not Raman scattering.

Data for the region from  $200$  to  $1000\text{ cm}^{-1}$  were acquired as the pressure was increased to  $16.18\text{ GPa}$ , where conditions were no longer hydrostatic (see Fig. 2). The pressure was then decreased to  $9.63\text{ GPa}$ . Data for the region from  $1000$  to  $1210\text{ cm}^{-1}$  were acquired as the pressure was decreased to  $1.39\text{ GPa}$  (see Fig. 3). Appearing in many of the spectra is a peak at  $1115\text{ cm}^{-1}$  that is attributable to an emission line of flat-screen monitors utilized in the laboratory, not a genuine Raman peak. No data were acquired above  $1210\text{ cm}^{-1}$  since earlier studies have shown that there are no peaks apparent at higher wavenumbers, and because of interference due to Raman scattering from the diamond line at  $\sim 1330\text{ cm}^{-1}$ .

## RESULTS AND DISCUSSION

Near  $3.2\text{ GPa}$ , spodumene undergoes a phase transition from  $C2/c$  to  $P2_1/c$ . This is evidenced by the dramatic change in the Raman spectrum. Although it is difficult to say definitely, it appears that some peaks split into two, some disappear altogether and several peaks appear at the transition (Figs 4 and 5).

Peaks  $\nu_8$ ,  $\nu_{21}$ ,  $\nu_{22}$ ,  $\nu_{24}$  and  $\nu_{29}$  appear through all pressures, although their positions shift with increasing pressure. Peaks  $\nu_6$ ,  $\nu_9$ ,  $\nu_{15}$  and  $\nu_{28}$  are not present above the transition. Peak  $\nu_4$  appears to split into  $\nu_3$  and  $\nu_4$ ,  $\nu_{13}$  into  $\nu_{11}$  and  $\nu_{14}$ ,  $\nu_{17}$  into  $\nu_{16}$  and  $\nu_{17}$ ,  $\nu_{19}$  into  $\nu_{19}$  and  $\nu_{20}$  and  $\nu_{26}$  into  $\nu_{25}$  and  $\nu_{27}$ . The following peaks appear at the phase transition:  $\nu_1$ ,

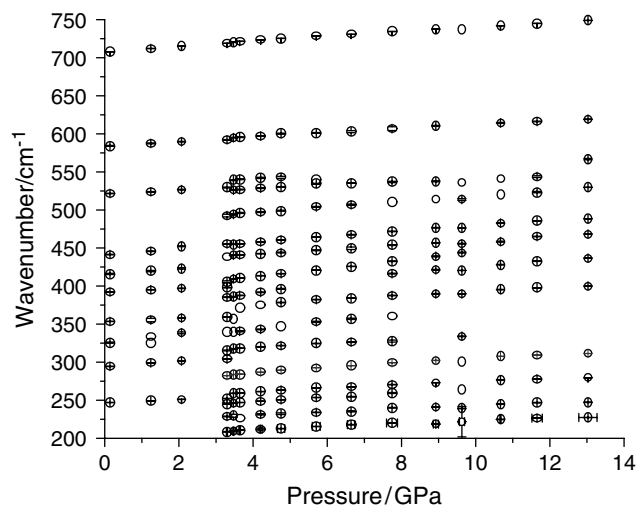


**Figure 4.** Plots of peak position as a function of pressure.

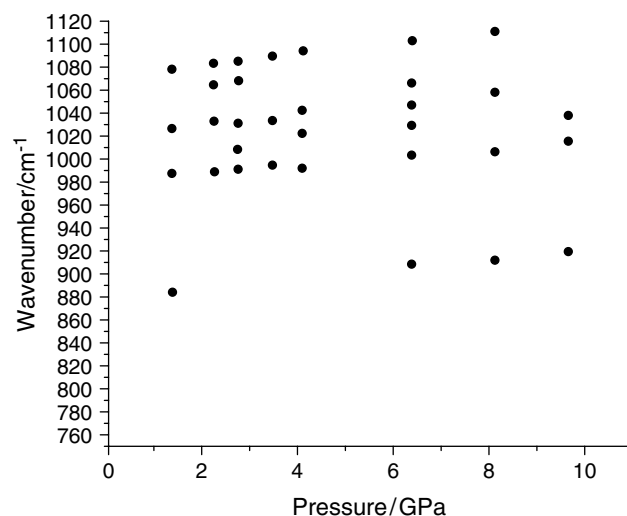


**Figure 5.** Plot of high-wavenumber peak positions as a function of pressure. Data acquired as pressure was decreased.

$\nu_2$ ,  $\nu_5$ ,  $\nu_7$ ,  $\nu_{10}$  and  $\nu_{18}$ . Peak  $\nu_{12}$  only appears after  $7.7\text{ GPa}$ . Peaks  $\nu_3$ ,  $\nu_7$ ,  $\nu_8$ ,  $\nu_{11}$ ,  $\nu_{14}$  and  $\nu_{20}$  do not appear through the highest pressures. The disappearance of these peaks might be evidence for a change in spodumene that may be associated with a second transition that retains the  $P2_1/c$  symmetry. Peak  $\nu_{24}$  is a very weak and broad peak. It is difficult to determine if this peak is constantly present, if it appears at the transition or if it is a Raman peak at all associated with the mineral. The wavenumber at which the peak appears shifts linearly with pressure, indicating that it may be a Raman peak. The authors suggest that this peak is due to the methanol–ethanol pressure medium, as there is a peak appearing in the ethanol spectrum at  $883\text{ cm}^{-1}$  and none appearing in the spectrum of spodumene at atmospheric pressure.

Prior to the phase transition, there were only 15 peaks apparent in the spectrum. According to factor group analysis, there should be a total of 30 peaks, 14 of  $A_g$  symmetry and 16 of  $B_g$  symmetry. Although no attempt was made in this experiment to discern the symmetries of the peaks, it is evident that too few appear. There are many reasons why the expected peaks may not be apparent, including accidental degeneracy (two peaks having the same energy, thereby appearing at the same wavenumber), two peaks having very close to the same energy with the resolution of the instrument being inadequate to distinguish between them, or the peaks could have too low an intensity to be above the noise of the measurement. Huang *et al.*<sup>9</sup> proposed that in a natural sample, disorder created by cation substitution might broaden the peaks, making them indistinct. This natural sample also exhibited fluorescence, which increased the noise of the measurement such that several peaks, known from previous studies to be present (especially in the 900–1200  $\text{cm}^{-1}$  region), are not apparent. The sample was investigated with excitation at 785 nm, and was found to fluoresce at this wavelength also.

With the destruction of the  $C_2$  site symmetry at the M1 and M2 positions, modes appear that were degenerate before the phase transition, especially in the low-wavenumber region of the spectrum. It is logical to assume that some of these

modes are directly related to vibrations involving the M2 atom. In this experiment,  $\nu_3$ ,  $\nu_{13}$ ,  $\nu_{17}$ ,  $\nu_{19}$  and  $\nu_{26}$  all appear to split, though  $\nu_{26}$  may actually be an appearance of a peak, not a splitting. In addition, the following modes appear, indicating that they also are related to M1 or M2 vibrations:  $\nu_1$ ,  $\nu_2$ ,  $\nu_5$ ,  $\nu_7$ ,  $\nu_{10}$  and  $\nu_{18}$ . This is not inconsistent with previous studies, which have assigned pyroxene bands appearing below 550  $\text{cm}^{-1}$  to cation translation, bending and stretching of bonds related to M1 and M2, and longer wavelength lattice modes.<sup>9,10–13</sup> Note that in the  $P2_1/c$  symmetry, there are two distinct silicate chains, which should contribute to an increase in number of modes observed as well, although most likely in the higher wavenumber region.

The spectrum of spodumene in the low-pressure phase can be compared with the Raman spectra of diopside,  $\text{CaMgSi}_2\text{O}_6$ , which is another pyroxene with  $C2/c$  symmetry.<sup>13,14</sup> At atmospheric pressure, diopside has eight bonds associated with the M2 site, whereas spodumene has six. Chopelas and Serghiou<sup>13</sup> report that at high pressure, however, diopside may also have six bonds to the M2 site, although this is unconfirmed. Also note that in diopside, M2 is bonded to  $\text{O}_{31}$ ,  $\text{O}_{32}$ ,  $\text{O}_{33}$  and  $\text{O}_{34}$ , whereas in spodumene, M2 is bonded to  $\text{O}_{32}$  and  $\text{O}_{33}$ .

Figure 6 compares the spectra of diopside (bottom) and spodumene (top) in the  $C2/c$  phase at 1 atm. Both spectra

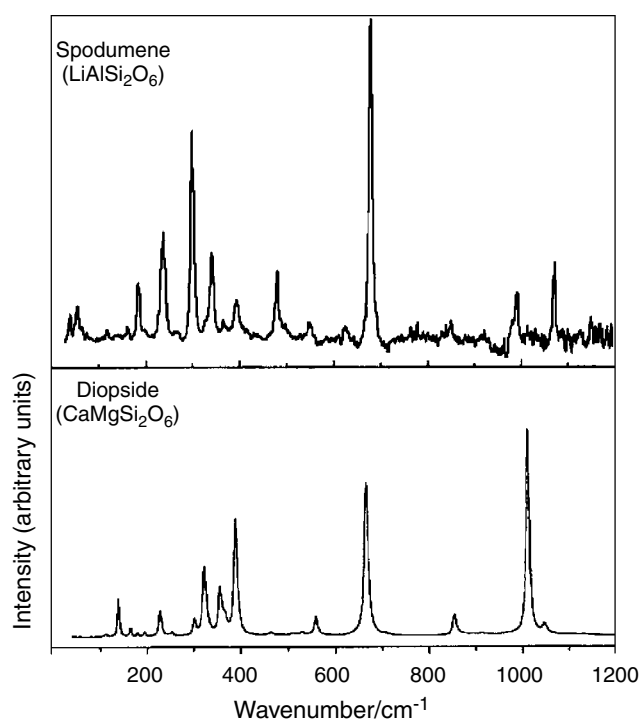


**Figure 6.** Top,  $C2/c$  spodumene on (110) face, and bottom,  $C2/c$  diopside on (110) face. Reference 19 assigns the vibrational regions in pyroxenes as follows: 800–1200  $\text{cm}^{-1}$  Si– $\text{O}_{\text{nb}}$  stretch, 650–800  $\text{cm}^{-1}$  Si– $\text{O}_{\text{b}}$  stretch, 425–650  $\text{cm}^{-1}$  Si–O bend and 50–425  $\text{cm}^{-1}$  complex lattice vibrations due to Si–O bend and M–O interactions.

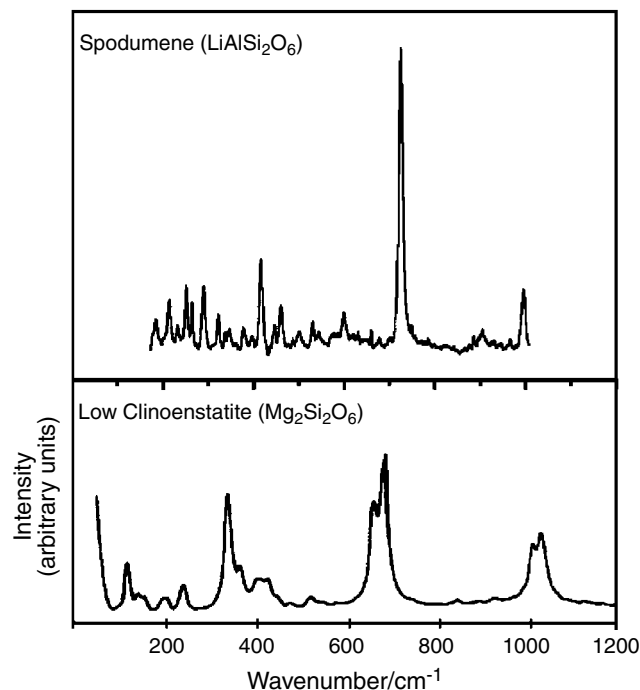


**Figure 7.**  $P2_1/c$  spodumene at 4.70 GPa (top) and  $P2_1/c$  low clinoenstatite ( $\text{Mg}_2\text{Si}_2\text{O}_6$ ) at 0 GPa (bottom, from reference 16 used with permission). Reference 19 assigns the vibrational regions in pyroxenes as follows: 800–1200  $\text{cm}^{-1}$  Si– $\text{O}_{\text{nb}}$  stretch, 650–800  $\text{cm}^{-1}$  Si– $\text{O}_{\text{b}}$  stretch, 425–650  $\text{cm}^{-1}$  Si–O bend and 50–425  $\text{cm}^{-1}$  complex lattice vibrations due to Si–O bend and M–O interactions.

have a singlet between 600 and 800  $\text{cm}^{-1}$  that is indicative of the  $C2/c$  phase in pyroxenes.<sup>9–11,15</sup> Both spectra have strong peaks near 140  $\text{cm}^{-1}$  and also have similar peaks in the 500–600  $\text{cm}^{-1}$  range, the Si—O chain bending region. Between 200 and 500  $\text{cm}^{-1}$  there is little similarity between the two spectra. The region above 1000  $\text{cm}^{-1}$ , where SiO stretching is found, is different in the two spectra, even though both spectra were acquired with laser light incident on the (110) face of the minerals. Peak intensities in this region have shown a strong dependence on crystal orientation. However, since the two minerals are oriented identically, this is not the explanation for the different number of peaks.

Above the transition, 23 peaks were observed. The following peaks appear to be indicative of a  $P2_1/c$  phase in spodumene:  $\nu_1, \nu_2, \nu_3, \nu_4, \nu_5, \nu_7, \nu_{10}, \nu_{12}, \nu_{14}, \nu_{16}$  and  $\nu_{18}$ . Although there are again too few peaks, there is a definite increase in the number of peaks, which indicates a decrease in symmetry of the crystal. Because the only change in bonding in this mineral is related to the Li—O3 bonds, any change in the spectrum should be attributable to those vibrations involving the M2 atom (Li) or the O3 atoms. Additionally, the peaks above 1000  $\text{cm}^{-1}$  were often difficult to discern after the transition because a broad peak appeared from 1050

to 1100  $\text{cm}^{-1}$ , which obscured any lower intensity peaks present (see Fig. 3).

Figure 7 shows a comparison between two pyroxenes of  $P2_1/c$  symmetry, spodumene (top) and low clinoenstatite ( $\text{MgSiO}_3$ ) (bottom).<sup>16</sup> In the 600–800  $\text{cm}^{-1}$  region for clinoenstatite a doublet appears, indicating two symmetrically distinct Si—O chains.<sup>9,15–17</sup> For spodumene, a singlet appears in this region throughout all pressures. In all other spectra of  $P2_1/c$  pyroxenes, there is a doublet in this region. It is difficult to compare the Si—O stretching region (above 800  $\text{cm}^{-1}$ ) because of the broad, indistinct peak that appeared in this region during our experiment. There appear to be similarities between 180 and 250  $\text{cm}^{-1}$ , but few other parallels between these two spectra are apparent.

Tables 1 and 2 show the observed change in wavenumbers with pressure (referred to as slope). Compression of the pyroxenes occurs primarily by the geometry change of M1 and M2 octahedra because the silica tetrahedra are relatively incompressible.<sup>17,18</sup> The M2 octahedra are more affected by this distortion than are the M1 octahedra,<sup>17</sup> hence a larger change in wavenumber with pressure indicates that the peak is likely to be associated with M2—O bonds. The peak that showed the largest change with pressure after the transition, peak  $\nu_{11}$ , was also one that disappeared near 8 GPa. The

**Table 1.** Peak positions (in  $\text{cm}^{-1}$ ) listed with pressure<sup>a</sup>

	0.141	1.243	2.071	3.295	3.47	3.638	4.203	4.754	5.702	6.640	7.745	8.927	9.630	10.668	11.654	13.026	Slope (pre-/post-)
$\nu_1$				209	209	211	212	213	216	218	220	219	222	225	227	227	1.86
$\nu_2$				229	230	227	232	232	234	235	240	241	239	245	247	247	2.01
$\nu_3$				245	246	247	249	251	254	255	260		264				2.90
$\nu_4$	247	249	251	252	259	260	261	263	266	267	271	273		277	278	279	1.63/2.20
$\nu_5$				282	284	284	287	290	293	295	299	302	301	308	309	311	2.90
$\nu_6$	295	299	302	304													2.89
$\nu_7$				315	317	318	320	322	325	326	328						2.56
$\nu_8$	326	334	339	340	340	341	343	347	352	357	360						4.50/4.92
$\nu_9$	354	355	358	359													1.92
$\nu_{10}$					357	371	375	378	382	384	388	390	390	395	398	400	3.50
$\nu_{11}$				385	386	388	392	396									7.59
$\nu_{12}$											416	421	421	428	433	437	4.16
$\nu_{13}$	392	395	397	398													1.92
$\nu_{14}$				406	410	411	414	416	421	426	433	439	444				5.44
$\nu_{15}$	416	420	423														3.63
$\nu_{16}$				439	441	441	443	444	447	450	454	457	456	458	465	468	2.77
$\nu_{17}$	441	446	452	455	455	455	458	461	464	467	472	477	476	483	485	488	4.61/3.58
$\nu_{18}$				493	494	496	497	499	504	507	510	514	514	521	523	530	3.55
$\nu_{19}$	522	524	527	530	526	527	529	530	534	535	537	538	536	541	544	567	2.61/2.90
$\nu_{20}$					539	540	542	543	540								0.54
$\nu_{21}$	584	587	590	592	595	596	597	600	601	603	607	611		614	616	619	2.60/2.52
$\nu_{22}$	708	712	715	719	721	722	723	725	729	731	734	738	738	742	745	749	3.49/2.88

<sup>a</sup> Error in peak position is  $<2 \text{ cm}^{-1}$ . Slope is change in Raman shift with pressure in  $\text{cm}^{-1} \text{ GPa}^{-1}$ . First number is pre-transition (0–3.47 GPa), second is post-transition (3.47–13.03 GPa).

**Table 2.** Long-wavenumber (in  $\text{cm}^{-1}$ ) peak position data

	1.386	2.254	2.78	3.467	4.1	6.388	8.107	9.63	Slope (pre-/post-)
$\nu_{23}$	885					908	911	918	3.11
$\nu_{24}$	987	989	991	995	992	1003	1007	1014	3.44/3.41
$\nu_{25}$			1008		1022	1029		1038	2.95
$\nu_{26}$	1027	1033	1031	1033					2.85
$\nu_{27}$					1043	1046	1058		4.62
$\nu_{28}$		1064	1068			1066			7.16
$\nu_{29}$	1079	1083	1085	1089	1094	1103	1112		5.00/4.68

fact that its position changed so dramatically with pressure and that  $\nu_{11}$  disappeared indicate that this peak is closely associated with an M2—O3 bond.

Between 8 and 10 GPa there is another change to the Raman spectrum of spodumene. Peaks  $\nu_3$ ,  $\nu_7$ ,  $\nu_{10}$  and  $\nu_{18}$  are no longer apparent above 10 GPa and a peak at  $416 \text{ cm}^{-1}$  appears. It is possible that these changes in the spectrum can be attributed to the formation of a new Li—O3 bond to O3<sub>4</sub>, while retaining the  $P2_1/c$  symmetry. This possibility must be investigated further. Chopelas and Serghiou<sup>13</sup> recently reported a similar change in the Raman spectrum of diopside ( $\text{CaMgSi}_2\text{O}_6$ ), which they attribute to a  $C2/c$  to  $C2/c$  change. The disappearance of some peaks and the appearance of others demonstrate this change. It is therefore likely that at high pressures other pyroxenes undergo similar changes that are apparent in the Raman spectrum but do not necessarily change the symmetry of the mineral.

## CONCLUSIONS

The  $C2/c$  to  $P2_1/c$  phase transition in spodumene is clearly demonstrated by several distinctive spectral changes. Of

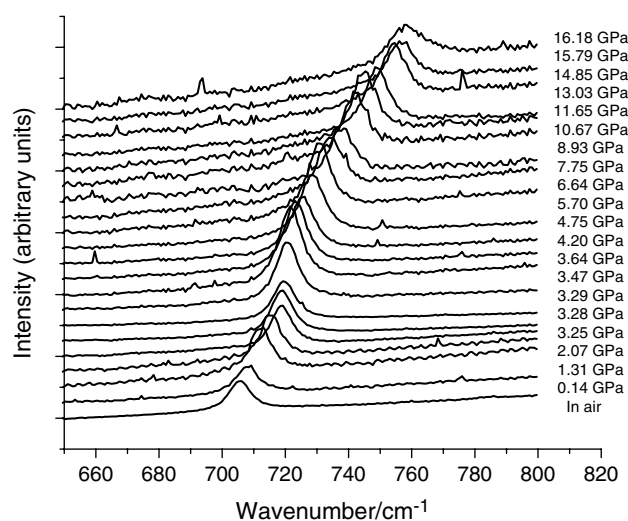


**Figure 8.** Silicate chain stretching peak through all pressures. No splitting or significant broadening, which would indicate a  $P2_1/c$  phase, is apparent above the transition.

particular note is the splitting of the  $250 \text{ cm}^{-1}$  peak into a doublet. Also, the appearance of a singlet instead of a doublet between  $600$  and  $800 \text{ cm}^{-1}$  in the  $P2_1/c$  phase appears to be unique to spodumene, as other  $P2_1/c$  pyroxenes display a doublet. The existence of the  $700 \text{ cm}^{-1}$  doublet has been attributed to two symmetrically distinct silicate chains and a singlet to two symmetrically equivalent chains.<sup>9,15–17</sup> If we accept this argument, then there is no Raman spectroscopic evidence that the transition creates symmetrically non-equivalent Si—O chains in spodumene. However, x-ray evidence indicates that there is a symmetry change to  $P2_1/c$ , so the interpretation must be incorrect. Other variations in the spectrum are consistent with a model of M2—O3 bond changes that leave M1—O and Si—O bonds intact. It could be argued that there are in fact two peaks present, but they are accidentally degenerate. X-ray diffraction studies show that the two silicate chains are symmetrically distinct, but geometrically similar at the transition, while other  $P2_1/c$  pyroxenes have geometrically very different silicate chains near their transitions. Spodumene's Si—O3—Si bond angles are very similar in both silicate chains near the transition,  $\sim 134^\circ$ .<sup>7</sup> We can contrast this with clinoenstatite's bond angles of  $133$  and  $127^\circ$ . Other  $P2_1/c$  pyroxenes display Si—O3—Si bond angles of  $141$  and  $139^\circ$  in  $\text{LiScSi}_2\text{O}_6$ ,  $140^\circ$  in both chains for  $\text{LiGeSi}_2\text{O}_6$ ,  $129$  and  $138^\circ$  in  $\text{Fe}_2\text{Si}_2\text{O}_6$  and  $138$  and  $129^\circ$  in  $\text{Zn}_2\text{Si}_2\text{O}_6$ . The argument could be made that because of their geometric similarity, the two silicate chains' vibrational bands would lie on top of one another. However, as the pressure is increased in spodumene, the similarity of the chains decreases. At  $8.8 \text{ GPa}$ , the bond angles are  $131$  and  $128^\circ$  and above this pressure they should continue to decrease in similarity.<sup>7</sup> A broadening of the Raman peak should have occurred because of this difference, but no evidence of such broadening appears (Fig. 8). In addition, previous studies which assign the doublet to singlet change in the spectrum to the Si—O chains utilized samples containing iron,<sup>9–11</sup> except for studies on enstatite ( $\text{MgCaSi}_2\text{O}_6$ ).<sup>15</sup> Spodumene ( $\text{LiAlSi}_2\text{O}_6$ ) and jadeite ( $\text{NaAlSi}_2\text{O}_6$ ) both display singlets whereas Li-aegirine ( $\text{LiFeSi}_2\text{O}_6$ ) and aegirine ( $\text{NaFe}^{2+}\text{Si}_2\text{O}_6$ ) both display doublets at low pressures, even though all of these are in the  $C2/c$  phase (Fig. 9). Clearly, the presence of a doublet is not indicative of the  $P2_1/c$  phase in all pyroxenes.

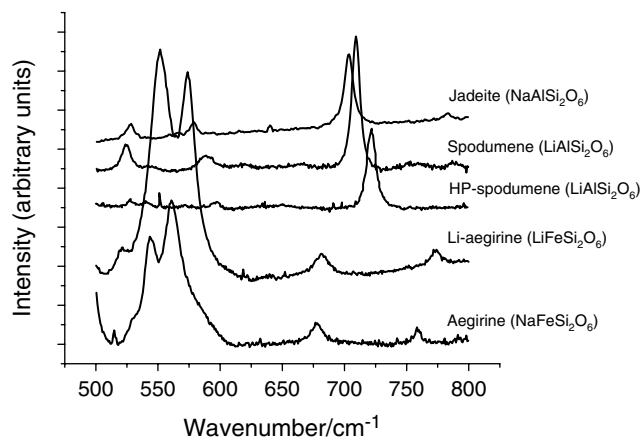


**Figure 9.** Strong doublets appear in the spectra of  $C2/c$  aegirine ( $\text{NaFeSi}_2\text{O}_6$ ) and  $C2/c$  Li-aegirine ( $\text{LiFeSi}_2\text{O}_6$ ), but not in  $P2_1/c$  spodumene (high-pressure  $\text{LiAlSi}_2\text{O}_6$ ),  $C2/c$  spodumene (low-pressure  $\text{LiAlSi}_2\text{O}_6$ ), or  $C2/c$  jadeite ( $\text{NaAlSi}_2\text{O}_6$ ).

Furthermore, another set of spectral changes appearing around 7.7 GPa might be indicative of a second transition. A recent study by Downs<sup>2</sup> shows that a transition to  $C2/c$ , but with M2 bonded to  $\text{O}3_1$  and  $\text{O}3_4$  instead of  $\text{O}3_2$  and  $\text{O}3_3$ , is expected upon continued increase in pressure following a  $P2_1/c$  to  $P2_1/c$  bonding change. The second set of changes in the Raman spectrum of spodumene observed in this study may be indicative of the first step ( $P2_1/c$  to  $P2_1/c$ ) of the phase transition back to  $C2/c$ .

Future investigations into the bonding characteristics of spodumene will include the calculation of force constants and utilizing this information to calculate the wavenumbers of all Raman modes in spodumene. A Raman study on an oriented crystal has been conducted to elucidate further the assignment of peaks, especially in the region below  $600\text{ cm}^{-1}$ .

## REFERENCES

1. Maaloe S, Aoki K. *Contrib. Mineral. Petrol.* 1977; **63**: 161.
2. Downs RT. *Am. Mineral.* 2003; **88**: 556.
3. Revenaugh J, Jordan TH. *J. Geophys. Res.* 1991; **96**: 19781.
4. Woodland AB. *Geophys. Res. Lett.* 1998; **25**: 1241.
5. Downs RT, Gibbs GV, Boisen MB Jr. *EOS Trans. Am. Geophys. Union* 1999; **80**: F1140.
6. Sharma SK, Simons B. *Am. Mineral.* 1981; **66**: 118.
7. Arlt T, Angel RJ. *Phys. Chem. Miner.* 2000; **27**: 719.
8. Mao HK, Bell PM, Shaner JW, Steinberg DJ. *J. Appl. Phys.* 1978; **49**: 3276.
9. Huang E, Chen CH, Huang T, Lin EH. *Am. Mineral.* 2000; **85**: 473.
10. Mernagh TP, Hoatson DM. *J. Raman Spectrosc.* 1997; **28**: 647.
11. Wang A, Jolliff BL, Haskin LA, Kuebler KE, Viskupic KM. *Am. Mineral.* 2001; **85**: 790.
12. Ghose S, Choudhury N, Chaplot SL, Chowdhury CP, Sharma SK. *Phys. Chem. Miner.* 1994; **20**: 469.
13. Chopelas A, Serghiou G. *Phys. Chem. Miner.* 2002; **29**: 403.
14. Ohlert JM, Chopelas A. *Trans. Am. Geophys. Union* 1999; **80**: F928.
15. Ross NL, Reynard B. *Eur. J. Mineral.* 1999; **11**: 585.
16. Mao H, Hemley RJ, Chao ECT. *Scanning Microsc.* 1987; **1**: 495.
17. Yang H, Finger LW, Conrad PG, Prewitt CT, Hazen RM. *Am. Mineral.* 1999; **84**: 245.
18. Chopelas A. *Am. Mineral.* 1999; **84**: 233.
19. Zhang L, Redhammer GJ, Salje EKH, Mookherjee M. *Phys. Chem. Miner.* 2002; **29**: 609.